

A preconditioned inverse iteration with an improved convergence guarantee

Foivos Alimisis¹, Daniel Kressner², Nian Shao^{2*},
Bart Vandereycken¹

¹Section of Mathematics, University of Geneva Geneva, 1205, Switzerland.

^{2*}Institute of Mathematics, EPFL, Lausanne, 1015, Switzerland.

*Corresponding author(s). E-mail(s): nian.shao@epfl.ch;

Contributing authors: foivos.alimisis@unige.ch; daniel.kressner@epfl.ch;
bart.vandereycken@unige.ch;

Abstract

Preconditioned eigenvalue solvers offer the possibility to incorporate preconditioners for the solution of large-scale eigenvalue problems, as they arise from the discretization of partial differential equations. The convergence analysis of such methods is intricate. Even for the relatively simple preconditioned inverse iteration (PINVIT), which targets the smallest eigenvalue of a symmetric positive definite matrix, the celebrated analysis by Neymeyr is highly nontrivial and only yields convergence if the starting vector is fairly close to the desired eigenvector. In this work, we prove a new non-asymptotic convergence result for a variant of PINVIT. Our proof proceeds by analyzing an equivalent Riemannian steepest descent method and leveraging convexity-like properties. We show a convergence rate that nearly matches the one of PINVIT. As a major benefit, we require a condition on the starting vector that tends to be less stringent. This improved global convergence property is demonstrated for two classes of preconditioners with theoretical bounds and a range of numerical experiments.

1 Introduction

Given a large-scale, symmetric positive definite (SPD) matrix $A \in \mathbb{R}^{n \times n}$ with eigenvalues $0 < \lambda_1 < \lambda_2 \leq \dots \leq \lambda_n$, this work considers the task of approximating the smallest eigenvalue λ_1 and an associated eigenvector u_* . Inverse iteration [8, Sec. 8.2.2] addresses this task by applying the power method to the inverse: $u_{t+1} = A^{-1}u_t$,

combined with some normalization to avoid numerical issues. This iteration inherits the excellent global convergence guarantee of the power method [8, Thm. 8.2.1]: For *almost every* choice of starting vector u_0 , the angle between u_* and u_t converges linearly to zero with rate λ_1/λ_2 . Moreover, the Rayleigh quotient $\lambda(u_t) := u_t^\top A u_t / u_t^\top u_t$ converges linearly to λ_1 with rate λ_1^2/λ_2^2 .

A major limitation of the inverse iteration is that it requires to solve a linear system with A in every iteration. Using, for example, a sparse Cholesky factorization of A for this purpose may become expensive unless A has a favorable sparsity pattern. In many situations, it is much cheaper to apply B^{-1} instead of A^{-1} for a preconditioner B constructed, for example, from multigrid methods [7], domain decomposition [24] or spectral sparsification [12]. In principle, the availability of a preconditioner allows for the use of an iterative solver, such as the preconditioned conjugate gradient method [8, Sec. 11.5.2], for solving the linear systems with A within inverse iteration. However, combining iterative methods in such an inner-outer iteration typically incurs redundancies. Instead, it is preferable to incorporate the preconditioner more directly, in a *preconditioned eigenvalue solver*.

The fruitfly of preconditioned eigenvalue solvers is the Preconditioned INVerse ITERation (PINVIT)

$$u_{t+1} = u_t - B^{-1}r_t \quad \text{with} \quad r_t = Au_t - \lambda(u_t)u_t. \quad (1)$$

While PINVIT can be viewed as a preconditioned steepest descent method for minimizing the Rayleigh quotient, Neymeyr's seminal (non-asymptotic) convergence analysis [15, 16] is based on interpreting (1) as a perturbed inverse iteration. *Assuming* that $\lambda(u_t) \in [\lambda_1, \lambda_2)$, a convergence result by Knyazev and Neymeyr [10, Thm. 1] states that

$$\frac{\lambda(u_{t+1}) - \lambda_1}{\lambda_2 - \lambda(u_{t+1})} \leq \rho^2 \frac{\lambda(u_t) - \lambda_1}{\lambda_2 - \lambda(u_t)}, \quad (2)$$

with the convergence rate determined by $\rho = 1 - (1 - \rho_B)(1 - \lambda_1/\lambda_2)$, where ρ_B is such that

$$\|I - B^{-1}A\|_A \leq \rho_B < 1. \quad (3)$$

Here and in the following, $\|\cdot\|_C$ denotes the vector and operator norms induced by an SPD matrix C . If $\rho_B \ll 1$, this result shows that PINVIT nearly attains the convergence rate of inverse iteration. In principle, the condition (3) can always be satisfied for any SPD matrix B by suitably rescaling B to B/η , which is equivalent to adding a step size $\eta > 0$ to PINVIT: $u_{t+1} = u_t - \eta B^{-1}r_t$. With PINVIT being one of the simplest preconditioned eigenvalue solvers, its analysis also provides important insights into the performance of more advanced methods like LOBPCG [9] and PRIMME [23]. Recently, provable accelerations of PINVIT, in the sense of Nesterov's accelerated gradient descent [14], have been introduced in [20, 21], based on certain convexity structures of the Rayleigh quotient. The analysis of these methods requires conditions on the initial vector that are even stricter than the one required for PINVIT.

If $\lambda(u_0) \in [\lambda_1, \lambda_2)$ then (1) implies that $\lambda(u_t) \in [\lambda_1, \lambda_2)$ is satisfied for all subsequent iterates u_t of PINVIT and u_t converges to u_* (in terms of angles). However, this assumption on the initial vector u_0 is quite restrictive. In fact, for a Gaussian random

initial u_0 , the probability of achieving $\lambda(u_0) < \lambda_2$ quickly vanishes for larger n and does not benefit from the quality of the preconditioner B . This is in stark contrast to both, inverse iteration ($B = A$) and steepest descent [4] ($B = I$), which converge to u_* almost surely for a Gaussian random initial vector.

In this work, we attain a new non-asymptotic convergence result for a slight variation of PINVIT. For this purpose, we first reformulate the task of computing the smallest eigenvalue and eigenvector as an equivalent Riemannian optimization problem on the unit sphere \mathbb{S}^{n-1} in \mathbb{R}^n , with the preconditioner B incorporated. A similar but different reformulation was used in [20]. We show that standard Riemannian steepest descent [22, Algorithm 3.1] applied to this problem coincides with a variant of PINVIT (1) that uses a different step size and normalization. Inspired by [4], we then establish and leverage a weaker notion of convexity (called weak-quasi-strong-convexity) to prove our main result, [Theorem 11](#): Riemannian steepest descent and, hence, our variant of PINVIT converge if the initial vector u_0 satisfies

$$\frac{u_0^\top B u_*}{\|u_0\|_B \|u_*\|_B} > \cos \varphi, \quad (4)$$

where φ is an angle measuring the distortion of the Euclidean geometry induced by the preconditioner at u_* ; see (13) for the precise definition. The convergence is linear and we prove an asymptotic convergence rate that matches (2) up to a small factor.

For $B = I$ and $B = A$, it holds that $\cos \varphi = 0$ and, thus, the condition (4) recovers the excellent global convergence properties of steepest descent and inverse iteration mentioned above. The practical use of PINVIT is between these two extreme scenarios and in such cases our numerical results indicate that the condition (4) is less stringent than $\lambda(u_0) < \lambda_2$. For the specific choices of mixed-precision and domain decomposition preconditioners, we provide theoretical results underlining that good preconditioners lead to $\cos \varphi \approx 0$.

2 PINVIT as steepest descent

The results of this work are based on a novel formulation of PINVIT as (Riemannian) steepest descent on \mathbb{S}^{n-1} . For this purpose, we define the following optimization problem for SPD matrices $A, B \in \mathbb{R}^{n \times n}$:

$$\min_{x \in \mathbb{S}^{n-1}} f(x), \quad f(x) := -\frac{x^\top B^{-1} x}{x^\top B^{-1/2} A B^{-1/2} x}. \quad (5)$$

Using the substitution $u = B^{-1/2} x$, we have that

$$f(x) = -\frac{u^\top u}{u^\top A u}.$$

The minimum of f is hence $-1/\lambda_1$ and is attained at $x_* = \frac{B^{1/2} u_*}{\|B^{1/2} u_*\|}$ for an eigenvector u_* belonging to the eigenvalue λ_1 of A , where $\|\cdot\|$ denotes the Euclidean norm.

The formulation (5) is inspired by the previous work [20], which considers the minimization of $-1/f(x)$ instead of $f(x)$. These two optimization problems are clearly equivalent and behave very similarly close to the optimum x_* . For a local convergence analysis, as the one performed in [20], the choice between the two optimization problems does not make a significant difference. For attaining results of a more global nature, this choice matters and it turns out that our new formulation (5) is more suitable.

Remark 1. *Our work also applies to generalized eigenvalue problems of the form $A - \lambda M$, for SPD matrices A and M . The additional matrix M can be absorbed by setting $\hat{A} = M^{-1/2}AM^{-1/2}$, $\hat{B} = M^{-1/2}BM^{-1/2}$ and $\hat{x} = \hat{B}^{-1/2}M^{-1/2}B^{1/2}x$, and one obtains the same type of optimization problem (5), simply with A, B and x replaced by \hat{A}, \hat{B} and $\hat{x}/\|\hat{x}\|$.*

We view \mathbb{S}^{n-1} as a Riemannian submanifold of \mathbb{R}^n with the restricted Euclidean metric. Minimizing (5) by the *Riemannian steepest descent* method yields the recurrence

$$x_{t+1} = \exp_{x_t}(-\eta_t \text{grad } f(x_t)), \quad (6)$$

for an initial vector $x_0 \in \mathbb{S}^{n-1}$, where grad denotes the Riemannian gradient on the sphere and \exp_{x_t} denotes the exponential map at x_t on \mathbb{S}^{n-1} (see below for explicit formulas). We impose the natural restriction

$$0 < \eta_t < \frac{\pi}{2\|\text{grad } f(x_t)\|} \quad (7)$$

on the step size.

The following proposition shows that the recurrence (6) is a variant of PINVIT (1) that uses a different step size¹ and normalization.

Proposition 2. *Consider the iterates x_t produced by the recurrence (6) with a step size satisfying (7). Then the transformed vectors $u_t := B^{-1/2}x_t$ satisfy the recurrence*

$$u_{t+1} = \beta_{t+1}(u_t - \eta_t^* B^{-1}r_t), \quad (8)$$

with a certain step size $\eta_t^* > 0$, a normalization $\beta_{t+1} > 0$ chosen such that $\|u_{t+1}\|_B = 1$, and the residual $r_t = Au_t - \lambda(u_t)u_t$.

Proof. A direct calculation of the Euclidean gradient of f shows

$$\nabla f(x_t) = -\frac{2(B^{-1}x_t + f(x_t)B^{-1/2}AB^{-1/2}x_t)}{\|A^{1/2}B^{-1/2}x_t\|^2}. \quad (9)$$

Because $I - x_t x_t^\top$ is the orthogonal projection to the tangent space of the sphere at x_t , the Riemannian gradient is given by (see, e.g., [1, Example 3.6.1])

$$\text{grad } f(x_t) = (I - x_t x_t^\top) \nabla f(x_t) = \nabla f(x_t), \quad (10)$$

¹Recall that PINVIT can use step size 1 thanks to the normalization of the preconditioner implied by (3).

where the latter equality follows from $x_t^\top \nabla f(x_t) = 0$. In particular, this implies that $\text{grad } f(x_t)$ is zero if and only if the residual r_t is zero. In this case, the recurrence (8) holds trivially. We may therefore assume $\text{grad } f(x_t) \neq 0$ in the following.

Using the explicit expression of the exponential map on the sphere from [1, Example 5.4.1], the recurrence (6) is rewritten as

$$\begin{aligned} x_{t+1} &= \cos(\|\eta_t \text{grad } f(x_t)\|)x_t - \sin(\|\eta_t \text{grad } f(x_t)\|) \frac{\text{grad } f(x_t)}{\|\text{grad } f(x_t)\|} \\ &= \beta_{t+1}(x_t - \bar{\eta}_t \text{grad } f(x_t)), \end{aligned}$$

where we set

$$\beta_{t+1} := \cos(\|\eta_t \text{grad } f(x_t)\|) \quad \text{and} \quad \bar{\eta}_t := \frac{\tan(\|\eta_t \text{grad } f(x_t)\|)}{\|\text{grad } f(x_t)\|}.$$

By (7), $\bar{\eta}_t$ is well defined and positive. Substituting $u_t = B^{-1/2}x_t$ and using (9) and (10), we obtain that

$$\begin{aligned} u_{t+1} &= \beta_{t+1} \left(u_t + \frac{2\bar{\eta}_t}{\|A^{1/2}B^{-1/2}x_t\|^2} (B^{-1}u_t + f(x_t)B^{-1}Au_t) \right) \\ &= \beta_{t+1} \left(u_t + \frac{2\bar{\eta}_t}{u_t^\top Au_t} \left(B^{-1}u_t - \frac{1}{\lambda(u_t)} B^{-1}Au_t \right) \right) \\ &= \beta_{t+1}(u_t - \eta_t^* B^{-1}r_t), \end{aligned}$$

with

$$\eta_t^* := \frac{2\bar{\eta}_t u_t^\top u_t}{(u_t^\top Au_t)^2} = \frac{2 \tan(\|\eta_t \text{grad } f(x_t)\|) u_t^\top u_t}{\|\text{grad } f(x_t)\| (u_t^\top Au_t)^2} > 0.$$

By definition, x_{t+1} is on the sphere and, therefore, it follows immediately that $\|u_{t+1}\|_B = 1$. \square

3 Quality of preconditioner

In this section, we discuss quantities that measure the quality of the preconditioner B in the context of preconditioned eigenvalue solvers.

3.1 Global: spectral equivalence

For any SPD matrices A, B , there exist constants $0 < \nu_{\min} \leq \nu_{\max}$ such that

$$\nu_{\min}(x^\top Bx) \leq x^\top Ax \leq \nu_{\max}(x^\top Bx), \quad \forall x, \quad (11)$$

a property sometimes called spectral equivalence. Equivalently,

$$\nu_{\min}\|x\|^2 \leq \|A^{1/2}B^{-1/2}x\|^2 \leq \nu_{\max}\|x\|^2, \quad \forall x. \quad (12)$$

The tightest bounds are obtained by choosing ν_{\min} and ν_{\max} as the smallest and largest eigenvalues of AB^{-1} , respectively. As we will see below, their ratio $\kappa_\nu := \nu_{\max}/\nu_{\min}$ determines the convergence rate of PINVIT and other preconditioned eigenvalue solvers.

While (11) can always be satisfied, ideally κ_ν is not too large. In particular, when A arises from the discretization of a partial differential equation, a good preconditioner B keeps κ_ν bounded as the discretization is refined; see also Section 5.

The inequality (11) only implies the condition (3) required by the convergence (analysis) of PINVIT when B is *scaled* in a suitable manner. According to [17], preconditioning with ηB^{-1} instead of B^{-1} with $\eta = 2/(\nu_{\max} + \nu_{\min})$ leads to $\rho_B = (\kappa_\nu - 1)/(\kappa_\nu + 1) < 1$ in (3).

3.2 Local: angle of distortion

Our condition on the initial vector will be based on an *angle of distortion* φ , which measures the distortion induced by the preconditioner at the eigenvector u_* :

$$\varphi := \arcsin \frac{\|u_*\|^2}{\|u_*\|_B \|u_*\|_{B^{-1}}} \in (0, \pi/2]. \quad (13)$$

For the vector $x_* = \frac{B^{1/2}u_*}{\|B^{1/2}u_*\|}$, we have that

$$\frac{x_*^\top B^{-1}x_*}{\|x_*\| \|B^{-1}x_*\|} = \frac{\|u_*\|^2}{\|u_*\|_B \|u_*\|_{B^{-1}}} = \sin \varphi.$$

In other words, φ is complementary to the angle between x_* and $B^{-1}x_*$, as illustrated in Figure 1.

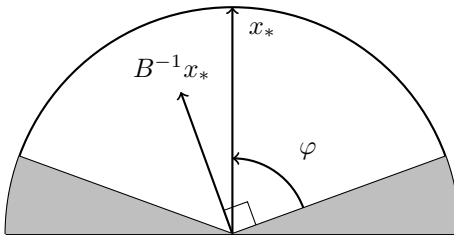


Fig. 1: Angle of distortion φ . Vectors x in the white region satisfy $\text{dist}(x, x_*) < \varphi$.

For $x \in \mathbb{S}^{n-1}$, we let

$$\text{dist}(x, x_*) := \arccos(x^\top x_*)$$

denote the angle between x_* and x , which happens to be the intrinsic Riemannian distance on the sphere. By suitably choosing the sign of x_* , we may always assume that $\text{dist}(x, x_*) \in [0, \pi/2]$. When $\text{dist}(x, x_*) < \varphi$, the following lemma establishes a lower bound on $x^\top B^{-1}x_*$ that will play an important role for the so-called weak-quasi-convexity property of the function f defined in (5); see Proposition 8 below.

Lemma 3. *With the notation introduced above, we have that*

$$x^\top B^{-1} x_* \geq \frac{\|u_*\|_{B^{-1}}^2}{\|u_*\|^2} \left(\cos(\text{dist}(x, x_*)) - \cos \varphi \right).$$

holds for any $x \in \mathbb{S}^{n-1}$ with $\text{dist}(x, x_*) < \varphi$.

Proof. Set $\sigma := \|u_*\|_{B^{-1}}^2 / \|u_*\|^2$. By the Cauchy–Schwarz inequality,

$$x^\top B^{-1} x_* = \sigma x^\top x_* + x^\top (B^{-1} - \sigma I) x_* \geq \sigma x^\top x_* - \|(B^{-1} - \sigma I) x_*\|.$$

On the other hand, it holds that

$$\frac{\|(B^{-1} - \sigma I) x_*\|^2}{\sigma^2} = \frac{\|B^{-1/2} u_* - \sigma B^{1/2} u_*\|^2}{\sigma^2 \|u_*\|_B^2} = 1 - \frac{\|u_*\|^4}{\|u_*\|_B^2 \|u_*\|_{B^{-1}}^2} = \cos^2 \varphi,$$

where the second equality follows by expanding the square. The result follows from combining the two relationships, using that $\cos(\text{dist}(x, x_*)) = x^\top x_*$. \square

In the absence of preconditioning, that is, $B = I$, the angle of distortion is $\varphi = \pi/2$ and the inequality of Lemma 3 becomes a trivial equality. The same holds when $B \neq I$ in the (unrealistic) scenario that u_* is also an eigenvector of B , which in particular holds when $B = A$. In the general case, one expects that φ is still close to $\pi/2$ or, equivalently, $\cos \varphi \approx 0$ for a good preconditioner B . From (11), one immediately obtains the bound

$$\cos^2 \varphi \leq 1 - \kappa_\nu^{-1}. \quad (14)$$

However, this bound is often not sharp and we will establish much tighter bounds for specific preconditioners in Section 6.

The following lemma provides a useful variational representation of $\cos \varphi$.

Lemma 4. *The angle of distortion φ satisfies*

$$\cos \varphi = \sup_{v^\top u_* = 0} \frac{v^\top B^{-1} u_*}{\|v\|_{B^{-1}} \|u_*\|_{B^{-1}}}. \quad (15)$$

Proof. The supremum in (15) is attained by the B^{-1} -orthogonal projection of u_* onto the subspace $\text{span}\{u_*\}^\perp$. This projection is given by the vector

$$v_* = u_* - \frac{\|u_*\|^2}{\|u_*\|_B^2} B u_*, \quad (16)$$

which follows from verifying that $v_*^\top u_* = 0$ and $v_*^\top B^{-1} (u_* - v_*) = \frac{\|u_*\|^2}{\|u_*\|_B^2} v_*^\top u_* = 0$.

Note that u_* , v_* and $u_* - v_*$ form a right triangle with respect to the B^{-1} -inner product, where u_* is the hypotenuse. By Pythagoras,

$$\frac{|v_*^\top B^{-1} u_*|^2}{\|v_*\|_{B^{-1}}^2 \|u_*\|_{B^{-1}}^2} = 1 - \frac{|(u_* - v_*)^\top B^{-1} u_*|^2}{\|(u_* - v_*)\|_{B^{-1}}^2 \|u_*\|_{B^{-1}}^2} = 1 - \frac{\|u_*\|^4}{\|u_*\|_B^2 \|u_*\|_{B^{-1}}^2} = \cos^2 \varphi,$$

where we use the definition (16) of v_* in the second equality, and the definition (13) of φ in the third equality. \square

Remark 5. For the situation considered in this work, the definition of leading angle from [20, Definition 6] amounts to

$$\vartheta \equiv \vartheta(I_n, -1/\lambda_1; f) = \inf_{f(x) \leq -1/\lambda_1} \inf_{v^\top x = 0} \arccos\left(\frac{|v^\top B^{-1}x|}{\|v\|_{B^{-1}} \|x\|_{B^{-1}}}\right).$$

Similar to the proof of Lemma 4, one can show that

$$\vartheta = \arcsin \frac{\|u_*\|_B^2}{\|Bu_*\| \|u_*\|}.$$

Comparing with the definition of φ in (13), one observes that both ϑ and φ are angles between Bu_* and u_* , one with respect to the standard Euclidean inner product and the other with respect to the B^{-1} -inner product.

4 Convergence analysis

In this section, we study the convergence of the Riemannian steepest descent method (6) or, equivalently, the PINVIT-like method (8). Our analysis utilizes concepts developed in [2, 4] for analyzing non-preconditioned eigenvalue solvers. In particular, we will use *smoothness* and the so-called *weak-quasi-strong-convexity* of the objective function f defined in (5) to show that the distance of the iterates (6) to x_* contracts linearly.

4.1 Smoothness-type property

Our analysis requires the following smoothness-type property, parametrized by a function $\gamma(x) > 0$:

$$f(x) - f_* \geq \frac{1}{2\gamma(x)} \|\text{grad } f(x)\|^2, \quad \forall x \in \mathbb{S}^{n-1}, \quad (17)$$

where $f_* := f(x_*) = -1/\lambda_1$ denotes the minimum of f . Note that standard smoothness in (convex) optimization implies (17), but not vice versa.

Proposition 6. *The smoothness-type property (17) holds with*

$$\gamma(x) = \frac{\nu_{\max} \cdot (\lambda_1^{-1} - \lambda_n^{-1})}{\|A^{1/2}B^{-1/2}x\|^2}.$$

Proof. Using the transformation

$$y(x) := \frac{A^{1/2}B^{-1/2}x}{\|A^{1/2}B^{-1/2}x\|} \in \mathbb{S}^{n-1}, \quad (18)$$

we get

$$f(x) = \bar{f}(y(x)) := -y(x)^\top A^{-1}y(x). \quad (19)$$

with $\min_{y \in \mathbb{S}^{n-1}} \bar{f}(y) = f_* = -1/\lambda_1$. Since \bar{f} is the Rayleigh quotient for $-A^{-1}$, we can use the smoothness property derived in [4]:

$$f(x) - f_* = \bar{f}(y(x)) - f_* \geq \frac{1}{2(\lambda_1^{-1} - \lambda_n^{-1})} \|\text{grad } \bar{f}(y(x))\|^2. \quad (20)$$

It remains to phrase this property in terms of x instead of y .

By the chain rule, we have $df(x) = d\bar{f}(y(x)) dy(x)$, which implies

$$\text{grad } f(x) = dy^\top(x) \text{grad } \bar{f}(y) \quad \text{and} \quad \|\text{grad } f(x)\| \leq \|dy(x)\| \|\text{grad } \bar{f}(y)\|. \quad (21)$$

To lower bound the right-hand side of (20), we thus need to upper bound the spectral norm of $dy(x)$. Denote $C := A^{1/2}B^{-1/2}$. A direct calculation shows that

$$dy(x)v = \frac{Cv}{\|Cx\|} - Cx \frac{x^\top C^\top Cv}{\|Cx\|^3} = \frac{1}{\|Cx\|} \left(I - \frac{Cxx^\top C^\top}{\|Cx\|^2} \right) Cv$$

holds for any v . Taking the Euclidean norm and noticing that the matrix in parentheses is an orthogonal projector, we obtain

$$\|dy(x)v\| \leq \frac{\|Cv\|}{\|Cx\|} \leq \frac{\sqrt{\nu_{\max}}\|v\|}{\|A^{1/2}B^{-1/2}x\|}$$

and, hence, $\|dy(x)\| \leq \sqrt{\nu_{\max}}/\|A^{1/2}B^{-1/2}x\|$. Plugging this inequality into (21), we get

$$\|\text{grad } \bar{f}(y(x))\|^2 \geq \frac{\|A^{1/2}B^{-1/2}x\|^2}{\nu_{\max}} \|\text{grad } f(x)\|^2.$$

Together with the bound (20), this gives the desired inequality:

$$f(x) - f_* \geq \frac{\|A^{1/2}B^{-1/2}x\|^2}{2\nu_{\max}(\lambda_1^{-1} - \lambda_n^{-1})} \|\text{grad } f(x)\|^2. \quad \square$$

It is worth noting that Proposition 7 combined with (12) give the global bound

$$\gamma(x) \leq \kappa_\nu \cdot (\lambda_1^{-1} - \lambda_n^{-1}), \quad \forall x \in \mathbb{S}^{n-1}. \quad (22)$$

4.2 Quadratic growth

In this and the next section, we derive two properties of f that correspond to weakened notions of strong convexity. We recall that $\text{dist}(x_1, x_2)$ denotes the angle between two vectors x_1, x_2 . If $\|x_1\| = \|x_2\| = 1$, it follows from a simple geometrical argument that

$$\|x_1 - x_2\| \leq \text{dist}(x_1, x_2) \leq \frac{\pi}{2} \|x_1 - x_2\|. \quad (23)$$

Proposition 7. *The function f satisfies*

$$f(x) - f_* \geq \frac{\mu(x)}{2} \text{dist}^2(x, x_*), \quad \forall x \in \mathbb{S}^{n-1},$$

with

$$\mu(x) := \frac{8\nu_{\min} \cdot (\lambda_1^{-1} - \lambda_2^{-1}) \|u_*\|_B}{\pi^2 \|A^{1/2} B^{-1/2} x\| \|u_*\|_A}.$$

Proof. As in the proof of [Proposition 6](#), we apply the transformation $y(x)$ from [\(18\)](#) to obtain the transformed objective function \bar{f} in [\(19\)](#). By the quadratic growth of \bar{f} established in [\[4\]](#), we have

$$f(x) - f_* = \bar{f}(y(x)) - f_* \geq (\lambda_1^{-1} - \lambda_2^{-1}) \text{dist}^2(y(x), u_*). \quad (24)$$

It thus remains to lower bound $\text{dist}(y(x), u_*)$ in terms of $\text{dist}(x, x_*)$. For this purpose, we may assume $\|u_*\| = 1$ without loss of generality. We first rewrite

$$y(x) - u_* = A^{1/2} B^{-1/2} z \quad \text{with} \quad z = \frac{x}{\|A^{1/2} B^{-1/2} x\|} - B^{1/2} A^{-1/2} u_*.$$

Using [\(23\)](#), we obtain that

$$\text{dist}^2(y(x), u_*) \geq \|y(x) - u_*\|^2 = \|A^{1/2} B^{-1/2} z\|^2 \geq \nu_{\min} \|z\|^2. \quad (25)$$

Since $x_* = B^{1/2} u_* / \|u_*\|_B$ and $A^{-1/2} u_* = \lambda_1^{-1/2} u_*$, we can also write

$$z = \frac{x}{\|A^{1/2} B^{-1/2} x\|} - \frac{\|u_*\|_B}{\|u_*\|_A} x_*,$$

For any $\alpha_1, \alpha_2 \in \mathbb{R}$ and $x_1, x_2 \in \mathbb{S}^{n-1}$, it holds that

$$\|\alpha_1 x_1 - \alpha_2 x_2\|^2 = \alpha_1^2 + \alpha_2^2 - 2\alpha_1 \alpha_2 x_1^\top x_2 \geq \alpha_1 \alpha_2 \|x_1 - x_2\|^2.$$

Using [\(23\)](#) once more, we can therefore bound

$$\|z\|^2 \geq \frac{\|u_*\|_B}{\|A^{1/2} B^{-1/2} x\| \|u_*\|_A} \|x - x_*\|^2 \geq \frac{4\|u_*\|_B}{\pi^2 \|A^{1/2} B^{-1/2} x\| \|u_*\|_A} \text{dist}^2(x, x_*).$$

Combined with [\(24\)](#) and [\(25\)](#), we yields the inequality

$$f(x) - f_* \geq \frac{4\nu_{\min} (\lambda_1^{-1} - \lambda_2^{-1}) \|u_*\|_B}{\pi^2 \|A^{1/2} B^{-1/2} x\| \|u_*\|_A} \text{dist}^2(x, x_*),$$

which is the desired result. \square

By (12), the quantity $\mu(x)$ of Proposition 7 admits the constant lower bound

$$\mu(x) \geq \frac{8(\lambda_1^{-1} - \lambda_2^{-1})}{\pi^2 \kappa_\nu} =: \mu_0, \quad \forall x \in \mathbb{S}^{n-1}. \quad (26)$$

This shows that μ_0 -strong convexity implies the quadratic growth established by Proposition 7, with $\mu(x)$ replaced by the constant μ_0 . This constant features the key quantities in the classical convergence result (2): the spectral gap of A^{-1} measured by $\lambda_1^{-1} - \lambda_2^{-1}$ and the spectral equivalence (11) of the preconditioner measured by κ_ν .

4.3 Weak-quasi-convexity

We now establish our second convexity-like property that is essential for the analysis of the Riemannian steepest descent method (6). It quantifies how proceeding in the direction of the negative spherical gradient pushes the iterates towards the optimum. For this purpose, we recall that $P_x := I - xx^\top$ is the orthogonal projector on the tangent space of \mathbb{S}^{n-1} at $x \in \mathbb{S}^{n-1}$. The logarithmic map on \mathbb{S}^{n-1} admits the explicit expression (see, for example, [5, Example 10.20])

$$\log_x(x_*) = \text{dist}(x, x_*) \frac{P_x x_*}{\|P_x x_*\|}, \quad (27)$$

provided that $\text{dist}(x, x_*) < \pi/2$. This is the inverse of the exponential map on \mathbb{S}^{n-1} , that is, $\exp_x(\log_x(x_*)) = x_*$.

Proposition 8. *Suppose that $x \in \mathbb{S}^{n-1}$ satisfies $\text{dist}(x, x_*) < \varphi$ with the angle of distortion φ defined in (13). Then*

$$\langle \text{grad } f(x), -\log_x(x_*) \rangle \geq 2a(x)(f(x) - f(x_*)), \quad (28)$$

where $\langle \cdot, \cdot \rangle$ denotes the Euclidean inner product, and

$$a(x) := \frac{\lambda_1 \|u_*\|_{B^{-1}}^2 (\cos(\text{dist}(x, x_*)) - \cos \varphi)}{\|A^{1/2} B^{-1/2} x\|^2 \|u_*\|^2}.$$

Proof. To simplify notation, we set $\theta_x := \text{dist}(x, x_*)$. Because $\|P_x x_*\|^2 = 1 - (x^\top x_*)^2 = 1 - \cos^2 \theta_x$, we can write (27) as

$$\log_x(x_*) = \frac{\theta_x}{\sin \theta_x} P_x x_*.$$

As mentioned in the proof of Proposition 2, $\text{grad } f(x) = P_x \nabla f(x) = \nabla f(x)$. We therefore get

$$\langle \text{grad } f(x), -\log_x(x_*) \rangle = -\frac{\theta_x}{\sin \theta_x} \langle P_x \nabla f(x), P_x x_* \rangle = -\frac{\theta_x}{\sin \theta_x} \langle \nabla f(x), x_* \rangle.$$

Using the expression (9) for $\nabla f(x)$, $B^{-1/2}AB^{-1/2}x_* = \lambda_1 B^{-1}x_*$, and $f_* = -1/\lambda_1$, one gets

$$\langle \nabla f(x), x_* \rangle = -\frac{2\lambda_1 x^\top B^{-1}x_*}{\|A^{1/2}B^{-1/2}x\|^2}(f(x) - f_*).$$

Combining the two equations above gives

$$\langle \text{grad } f(x), -\log_x(x_*) \rangle = \frac{2\lambda_1 \theta_x (x^\top B^{-1}x_*)}{\|A^{1/2}B^{-1/2}x\|^2 \sin \theta_x}(f(x) - f_*).$$

The result now follows from the bound on $x^\top B^{-1}x_*$ established in Lemma 3, additionally using that $\theta_x / \sin \theta_x \geq 1$. \square

Remark 9. If $\cos(\text{dist}(x, x_*)) \geq \cos \varphi + c \sin^2 \varphi$ for some $0 < c < 1/2$, the factor $a(x)$ of Proposition 8 can be bounded by a constant:

$$a(x) \geq \frac{c \|u_*\|_A^2}{\|A^{1/2}B^{-1/2}x\|^2 \|u_*\|_B^2} \geq \frac{c}{\kappa_\nu},$$

This follows from (12), (13), and $Au_* = \lambda_1 u_*$.

4.4 Weak-quasi-strong-convexity

The quadratic growth and weak-quasi-convexity properties established above result in the following important property.

Proposition 10. *The function f defined in (5) satisfies*

$$f(x) - f_* \leq \frac{1}{a(x)} \langle \text{grad } f(x), -\log_x(x_*) \rangle - \frac{\mu(x)}{2} \text{dist}^2(x, x_*),$$

for every $x \in \mathbb{S}^{n-1}$ satisfying $\text{dist}(x, x_*) < \varphi$, with $\mu(x)$ and $a(x)$ defined in Propositions 7 and 8, respectively.

Proof. By Propositions 7 and 8,

$$\frac{\mu(x)}{2} \text{dist}^2(x, x_*) \leq f(x) - f_* \leq \frac{1}{2a(x)} \langle \text{grad } f(x), -\log_x(x_*) \rangle.$$

Note that $\text{dist}(x, x_*) < \varphi$ implies $a(x) > 0$. Applying this inequality twice shows the desired result:

$$\begin{aligned} f(x) - f_* &\leq \frac{1}{2a(x)} \langle \text{grad } f(x), -\log_x(x_*) \rangle + \frac{\mu(x)}{2} \text{dist}^2(x, x_*) - \frac{\mu(x)}{2} \text{dist}^2(x, x_*) \\ &\leq \frac{1}{a(x)} \langle \text{grad } f(x), -\log_x(x_*) \rangle - \frac{\mu(x)}{2} \text{dist}^2(x, x_*). \end{aligned} \quad \square$$

4.5 Convergence analysis

Theorem 11 below contains the main theoretical result of this work, on the contraction of the error (measured in terms of the angles $\text{dist}(x_t, x_*)$) for the iterates produced by the Riemannian steepest descent method for (5). The condition on the initial vector prominently features the angle of distortion φ defined in (13), whereas the contraction rate involves the relative eigenvalue gap for A^{-1} and the quantity $\kappa_\nu = \nu_{\max}/\nu_{\min}$ measuring the spectral equivalence (11) of the preconditioner.

Theorem 11. *For an eigenvector u_* associated with the smallest eigenvalue λ_1 and an SPD preconditioner B , let $x_* := B^{1/2}u_*/\|B^{1/2}u_*\|$. Apply the Riemannian steepest descent method (6) to the optimization problem (5), with a starting vector $x_0 \in \mathbb{S}^{n-1}$ such that*

$$\text{dist}(x_0, x_*) < \varphi, \quad (29)$$

and a step size η_t satisfying

$$\eta_t \leq \frac{a(x_t)}{\gamma(x_t)} = \frac{\lambda_1 \|u_*\|_{B^{-1}}^2 (\cos(\text{dist}(x_t, x_*)) - \cos \varphi)}{\nu_{\max} \|u_*\|^2 (\lambda_1^{-1} - \lambda_n^{-1})},$$

with $\gamma(x)$ and $a(x)$ defined in Propositions 6 and 8. Then the iterates x_t produced by (6) satisfy

$$\text{dist}^2(x_{t+1}, x_*) \leq (1 - \xi_t) \text{dist}^2(x_t, x_*),$$

where $\xi_t := \eta_t \mu(x_t) a(x_t)$ with $\mu(x)$ defined in Proposition 7, respectively. When fixing the step size $\eta_t = a(x_t)/\gamma(x_t)$ we have

$$\xi_t = \frac{8\lambda_1^2 \|u_*\|_B \|u_*\|_{B^{-1}}^4 (\cos(\text{dist}(x_t, x_*)) - \cos \varphi)^2}{\pi^2 \|u_*\|^4 \|u_*\|_A} \frac{\lambda_1^{-1} - \lambda_2^{-1}}{\|A^{1/2}B^{-1/2}x_t\|^3} \frac{\lambda_1^{-1} - \lambda_2^{-1}}{\kappa_\nu (\lambda_1^{-1} - \lambda_n^{-1})} \quad (30)$$

bounded below by a positive constant, and $\text{dist}(x_t, x_*)$ converges linearly to zero.

Proof. By (6), we have $\log_{x_t}(x_{t+1}) = -\eta_t \text{grad} f(x_t)$. Since $\text{dist}(x, y) = \|\log_x(y)\|$, it follows that

$$\begin{aligned} \text{dist}^2(x_{t+1}, x_*) &\leq \|-\eta_t \text{grad} f(x_t) - \log_{x_t}(x_*)\|^2 \\ &= \eta_t^2 \|\text{grad} f(x_t)\|^2 + \text{dist}^2(x_t, x_*) + 2\eta_t \langle \text{grad} f(x_t), \log_{x_t}(x_*) \rangle, \end{aligned} \quad (31)$$

where the inequality is a consequence [4, Proposition 16] of the Rauch comparison theorem. By Propositions 6 and 10, we have

$$\begin{aligned} \frac{1}{a(x_t)} \langle \text{grad} f(x_t), \log_{x_t}(x_*) \rangle &\leq f_* - f(x_t) - \frac{\mu(x_t)}{2} \text{dist}^2(x_t, x_*) \\ &\leq -\frac{1}{2\gamma(x_t)} \|\text{grad} f(x_t)\|^2 - \frac{\mu(x_t)}{2} \text{dist}^2(x_t, x_*). \end{aligned}$$

Multiplying with $2\eta_t a(x_t)$ and using the hypothesis $\eta_t \leq a(x_t)/\gamma(x_t)$, this gives

$$\begin{aligned} 2\eta_t \langle \text{grad } f(x_t), \log_{x_t}(x_*) \rangle &\leq -\frac{\eta_t a(x_t)}{\gamma(x_t)} \|\text{grad } f(x_t)\|^2 - \eta_t \mu(x_t) a(x_t) \text{dist}^2(x_t, x_*) \\ &\leq -\eta_t^2 \|\text{grad } f(x_t)\|^2 - \eta_t \mu(x_t) a(x_t) \text{dist}^2(x_t, x_*). \end{aligned}$$

Plugging this inequality into (31) proves the first part of the theorem:

$$\text{dist}^2(x_{t+1}, x_*) \leq (1 - \eta_t \mu(x_t) a(x_t)) \text{dist}^2(x_t, x_*).$$

The expression (30) directly follows from the definitions of $a(x_t)$, $\gamma(x_t)$, $\mu(x_t)$, implying $\text{dist}(x_t, x_*) \leq \text{dist}(x_0, x_*)$. Finally, the claimed linear convergence can be concluded from the fact that ξ_t admits the constant lower bound

$$\xi_t \geq \frac{8\lambda_1^2 \|u_*\|_B \|u_*\|_{B^{-1}}^4 (\cos(\text{dist}(x_0, x_*)) - \cos \varphi)^2}{\pi^2 \|u_*\|^4 \|u_*\|_A} \frac{\lambda_1^{-1} - \lambda_2^{-1}}{\nu_{\max}^{3/2}} \frac{1}{\kappa_\nu (\lambda_1^{-1} - \lambda_n^{-1})} > 0,$$

where we use $\text{dist}(x_t, x_*) \leq \text{dist}(x_0, x_*)$ and the spectral equivalence (12). \square

By Proposition 2, Theorem 11 establishes an error contraction, with contraction rate $1 - \xi_t$, also for the PINVIT-like method (8), if the step size restriction (7) is satisfied. Using the smoothness-type property (17) and the weak-quasi-convexity property (28), it follows that

$$\frac{a(x_t)}{\gamma(x_t)} \leq \frac{2a(x_t)(f(x_t) - f(x_*))}{\|\text{grad } f(x_t)\|^2} \leq \frac{-\langle \text{grad } f(x_t), \log_{x_t}(x_*) \rangle}{\|\text{grad } f(x_t)\|^2} < \frac{\pi}{2\|\text{grad } f(x_t)\|},$$

where the last inequality uses that $\|\log_{x_t}(x_*)\| = \text{dist}(x_t, x_*) < \pi/2$ is implied by (29). Hence, the step size restriction $\eta_t \leq a(x_t)/\gamma(x_t)$ imposed by Theorem 11 always implies (7). In terms of the PINVIT iterates $u_t = B^{-1/2}x_t$, the initial condition (29) takes the form

$$\text{dist}(x_0, x_*) = \text{dist}_B(u_0, u_*) := \arccos\left(\frac{u_0^\top B u_*}{\|u_0\|_B \|u_*\|_B}\right) < \varphi, \quad (32)$$

where the sign of u_* is chosen such that $u_0^\top B u_* \geq 0$.

The following corollary establishes convergence for a constant step size.

Corollary 12. *If*

$$\cos(\text{dist}(x_0, x_*)) \geq \cos \varphi + c \sin^2 \varphi \quad \text{and} \quad \eta = \frac{c}{\kappa_\nu^2 (\lambda_1^{-1} - \lambda_n^{-1})} \quad (33)$$

for some $0 < c < 1/2$, then the Riemannian steepest descent method (6) with step size η produces iterates x_t satisfying

$$\text{dist}^2(x_t, x_*) \leq \left(1 - \frac{8c^2(\lambda_1^{-1} - \lambda_2^{-1})}{\pi^2 \kappa_\nu^4 (\lambda_1^{-1} - \lambda_n^{-1})}\right)^t \text{dist}^2(x_0, x_*). \quad (34)$$

Thus, x_t converges linearly to x_* .

Proof. The proof proceeds by induction on t . The result for $t = 0$ is trivial. Suppose (34) holds for some $t \geq 1$ and we now show that it also holds for $t + 1$. From (33) and (34), it follows that

$$\cos(\text{dist}(x_t, x_*)) \geq \cos(\text{dist}(x_0, x_*)) \geq \cos \varphi + c \sin^2 \varphi.$$

As shown in (22) and Remark 9, we have $\gamma(x_t) \leq \kappa_\nu(\lambda_1^{-1} - \lambda_n^{-1})$ and $a(x_t) \geq c/\kappa_\nu$. Hence, the choice of η in (33) satisfies the condition $\eta \leq a(x_t)/\gamma(x_t)$. By Theorem 11,

$$\text{dist}^2(x_{t+1}, x_*) \leq (1 - \eta\mu(x_t)a(x_t)) \text{dist}^2(x_t, x_*).$$

Using the lower bound (26) on $\mu(x_t)$ and, once again, $a(x_t) \geq c/\kappa_\nu$, the contraction rate can be bounded by

$$1 - \eta\mu(x_t)a(x_t) \leq 1 - \eta \frac{8c(\lambda_1^{-1} - \lambda_2^{-1})}{\pi^2 \kappa_\nu^2} = 1 - \frac{8c^2(\lambda_1^{-1} - \lambda_2^{-1})}{\pi^2 \kappa_\nu^4 (\lambda_1^{-1} - \lambda_n^{-1})}.$$

This completes the induction step. \square

Corollary 12 immediately yields a statement on the iteration complexity.

Corollary 13. *Suppose that Riemannian steepest descent (6) is applied to 5 with starting vector x_0 and step size η satisfying (33). Then an approximation x_T of x_* such that $\text{dist}(x_T, x_*) \leq \epsilon$ is returned after*

$$T = \mathcal{O}\left(\frac{\kappa_\nu^4}{c^2} \frac{\lambda_1^{-1} - \lambda_n^{-1}}{\lambda_1^{-1} - \lambda_2^{-1}} \log \frac{\text{dist}(x_0, x_*)}{\epsilon}\right)$$

iterations.

The following lemma simplifies the condition on the starting vector in Corollary 12, at the expense of making it potentially (much) stricter.

Lemma 14. *If*

$$\cos^2(\text{dist}(x_0, x_*)) \geq 1 - \frac{1 - 2c}{\kappa_\nu}, \quad 0 < c < 1/2,$$

then the condition (33) on the starting vector x_0 is satisfied.

Proof. To establish the result, we show that $1 - \frac{1-2c}{\kappa_\nu} \geq (\cos \varphi + c \sin^2 \varphi)^2$ holds for every $0 < c < 1/2$. For this purpose, consider the quadratic function

$$\begin{aligned} q(c) &= (\cos \varphi + c \sin^2 \varphi)^2 - 1 + (1 - 2c)/\kappa_\nu \\ &= (\sin^4 \varphi)c^2 + 2(\cos \varphi \sin^2 \varphi - 1/\kappa_\nu)c + 1/\kappa_\nu - \sin^2 \varphi. \end{aligned}$$

By (14), we know that $q(0) = 1/\kappa_\nu - \sin^2 \varphi \leq 0$. At the same time, we have

$$q(1/2) = \frac{1}{4}\sin^4 \varphi + \cos \varphi \sin^2 \varphi - \sin^2 \varphi \leq 0.$$

Because q is quadratic with leading non-negative coefficient, it follows that $q(c) \leq 0$ for every $0 < c < 1/2$, which completes the proof. \square

We now derive the *asymptotic* convergence rate implied by Theorem 11. This asymptotic rate is much more favorable than the non-asymptotic rate established in Corollary 12.

Proposition 15. *For the Riemannian steepest descent method (6) with step size $\eta_t = a(x_t)/\gamma(x_t)$, the quantity ξ_t determining the convergence rate $1 - \xi_t$, according to Theorem 11, satisfies*

$$\xi_\infty := \lim_{t \rightarrow \infty} \xi_t = \frac{8}{\pi^2(1 + \cos \varphi)^2} \frac{\lambda_1^{-1} - \lambda_2^{-1}}{\kappa_\nu(\lambda_1^{-1} - \lambda_n^{-1})}.$$

Proof. Theorem 11 shows that $\text{dist}(x_t, x_*) \rightarrow 0$ as $t \rightarrow \infty$. Inserted into (30), this gives

$$\xi_\infty = \frac{8\lambda_1^2 \|u_*\|_B \|u_*\|_{B^{-1}}^4}{\pi^2 \|u_*\|_A^4 \|u_*\|_A} \frac{(1 - \cos \varphi)^2}{\|A^{1/2} B^{-1/2} x_*\|^3} \frac{\lambda_1^{-1} - \lambda_2^{-1}}{\kappa_\nu(\lambda_1^{-1} - \lambda_n^{-1})}.$$

Using the relations

$$\lambda_1^2 = \frac{\|u_*\|_A^4}{\|u_*\|_A^4}, \quad \|A^{1/2} B^{-1/2} x_*\|^3 = \frac{\|u_*\|_A^3}{\|u_*\|_B^3} \quad \text{and} \quad \sin \varphi = \frac{\|u_*\|^2}{\|u_*\|_B \|u_*\|_{B^{-1}}},$$

the expression for ξ_∞ simplifies to

$$\xi_\infty = \frac{8(1 - \cos \varphi)^2}{\pi^2 \sin^4 \varphi} \frac{\lambda_1^{-1} - \lambda_2^{-1}}{\kappa_\nu(\lambda_1^{-1} - \lambda_n^{-1})} = \frac{8}{\pi^2(1 + \cos \varphi)^2} \frac{\lambda_1^{-1} - \lambda_2^{-1}}{\kappa_\nu(\lambda_1^{-1} - \lambda_n^{-1})}. \quad \square$$

The convergence result (2) by Knyazev and Neymeyr shows that the *eigenvalue* approximations of PINVIT converge linearly with the asymptotic convergence rate ρ^2 . When B is optimally scaled, then

$$\rho = 1 - \frac{2}{\kappa_\nu + 1} \frac{\lambda_1^{-1} - \lambda_2^{-1}}{\lambda_1^{-1}};$$

see [Section 3.1](#). On the other hand, [Proposition 15](#) establishes the asymptotic convergence rate $1 - \xi_\infty$ for the *eigenvector* approximation error. As the eigenvalue approximation error is quadratic in the eigenvector approximation error (see, for example, [\[25, Eq. \(27.3\)\]](#)), it is reasonable to compare ξ_∞ with $1 - \rho$:

$$\xi_\infty = (1 - \rho) \cdot \frac{4}{\pi^2(1 + \cos \varphi)^2} \cdot \frac{\kappa_\nu + 1}{\kappa_\nu} \cdot (1 + \lambda_n^{-1}).$$

Because $0 \leq \cos \varphi < 1$, this shows that our asymptotic rate matches (up to a small constant) the sharp rate by Knyazev and Neymeyr.

5 Distortion angle for specific preconditioners

The convergence results of the previous section, most notably [Theorem 11](#), requires the condition [\(32\)](#) on the initial vector u_0 , which can be restated as

$$\frac{u_0^\top B u_*}{\|u_0\|_B \|u_*\|_B} > \cos \varphi = \sup_{v^\top u_* = 0} \frac{v^\top B^{-1} u_*}{\|v\|_{B^{-1}} \|u_*\|_{B^{-1}}}, \quad (35)$$

where u_* is an eigenvector belonging to the smallest eigenvalue λ_1 of A . For a (Gaussian) random vector u_0 , the left-hand side of [\(35\)](#) is nonzero almost surely, but it is unlikely to be far away from zero. Therefore, a good global convergence guarantee requires $\cos \varphi$ to be small. In this section, we will demonstrate for two specific types of preconditioners that $\cos \varphi$ can be close to zero under reasonable assumptions.

5.1 Additive Schwarz preconditioners

Domain decomposition methods (DDM) are widely used strategies for solving large-scale partial differential equations (PDEs). They are based on splitting a PDE, or an approximation of it, into coupled problems on smaller subdomains that collectively form a (possibly overlapping) partition of the original computational domain. A powerful way to analyze and develop DDM is through a subspace perspective [\[26\]](#) that divides the solution space into smaller subspaces, typically corresponding to the geometric structure of the subdomain partition. Here, we consider an additive Schwarz preconditioner as a representative DDM approach. Further details on DDM can be found in several classical references on the topic, such as [\[24\]](#). The following discussion builds on the previous work [\[20\]](#).

We first briefly describe a relatively standard mathematical setting for elliptic PDEs. On a convex polygonal domain $\Omega \subset \mathbb{R}^d$ with $d = 2$ or 3 , consider a symmetric and uniformly positive definite coefficient matrix $\{a_{ij}(x)\}_{i,j=1}^d$ such that $a_{ij}(x) \in C^{0,1}(\overline{\Omega})$ for $i, j = 1, \dots, d$. Let $V_H \subset V_h \subset H_0^1(\Omega)$ be continuous, piecewise linear finite element spaces based on quasi-uniform triangular partitions \mathcal{T}_H and \mathcal{T}_h of Ω , such that \mathcal{T}_h is a refinement of \mathcal{T}_H , and $0 < h < H < 1$ are the maximum mesh sizes of \mathcal{T}_h and \mathcal{T}_H , respectively. Then the elliptic PDE eigenvalue problem discretized on V_h takes

the following form:

$$\mathcal{A}(u_*, v) = \lambda_1 \langle u_*, v \rangle_2 \quad \forall v \in V_h, \quad \text{where } \|u_*\|_2 = 1 \text{ and } u_* \in V_h. \quad (36)$$

Here $\langle \cdot, \cdot \rangle_2$ and $\|\cdot\|_2$ denote the L^2 inner product and norm, respectively, and

$$\mathcal{A}(u, v) := \sum_{i,j=1}^d \int_{\Omega} a_{ij}(x) \frac{\partial u}{\partial x_i} \frac{\partial v}{\partial x_j} dx. \quad (37)$$

The global solver is the linear operator $A^{-1} : V_h \rightarrow V_h$ such that $u \mapsto A^{-1}u$ satisfies

$$\mathcal{A}(A^{-1}u, v) = \langle u, v \rangle_2 \quad \forall v \in V_h.$$

We are interested in an additive Schwarz preconditioner B^{-1} for A^{-1} .

To aid in understanding, we present a specific example of additive Schwarz preconditioners, following the structure outlined in [6, Section 7.4].

Example 1 (Two-level overlapping domain decomposition preconditioner). *Consider the region $\Omega = [0, 1]^2$. Let \mathcal{T}_H be a coarse triangulation as shown in Figure 2. The region Ω is divided into non-overlapping subdomains Ω_j for $1 \leq j \leq 16$, which are aligned with \mathcal{T}_H . Subsequently, \mathcal{T}_H is further subdivided to obtain the finer triangulation \mathcal{T}_h . Define $\tilde{\Omega}_j = \tilde{\Omega}_{j,\delta} \cap \bar{\Omega}$, where $\tilde{\Omega}_{j,\delta}$ is an open set obtained by enlarging Ω_j by a band of width δ , ensuring $\tilde{\Omega}_j$ is aligned with \mathcal{T}_h as shown in Figure 2. One often assumes that the overlapping ratio δ/H is bounded below by a constant, which is 0.5 in this case.*

Let $V_j \subset V_h$ denote the subspace of continuous, piecewise linear functions supported in $\tilde{\Omega}_j$ for $1 \leq j \leq 16$. Define the coarse/local solvers A_H^{-1} and A_j^{-1} through

$$\begin{aligned} \mathcal{A}(A_H^{-1}u_H, v_H) &= \langle u_H, v_H \rangle_2 \quad \forall v_H \in V_H, \\ \mathcal{A}(A_j^{-1}u_j, v_j) &= \langle u_j, v_j \rangle_2 \quad \forall v_j \in V_j. \end{aligned}$$

Then the two-level overlapping domain decomposition preconditioner is given by

$$B^{-1} = I_H A_H^{-1} I_H^\top + \sum_{j=1}^{16} I_j A_j^{-1} I_j^\top,$$

where $I_H : V_H \mapsto V_h$ and $I_j : V_j \mapsto V_h$ are the natural injection operators, i.e., $I_H v_H = v_H$ for all $v_H \in V_H$, and $I_j v_j = v_j$ for all $1 \leq j \leq 16$ and $v_j \in V_j$.

Under reasonable assumptions, such as those stated in [24, Assumptions 2.2–2.4], it holds that $\cos \varphi = \mathcal{O}(H)$ as $H \rightarrow 0$. To see this, we employ the following results from [20, Lemmas. 34 and 35], which hold under such assumptions:

$$\|B^{-1}u_* - \lambda_H^{-1}u_*\|_{\mathcal{A}} \leq c_d \lambda_1^{-1/2} H \quad \text{and} \quad \|v\|_{A^{-1}} \leq c_d \|v\|_{B^{-1}} \quad \forall v \in V_h, \quad (38)$$

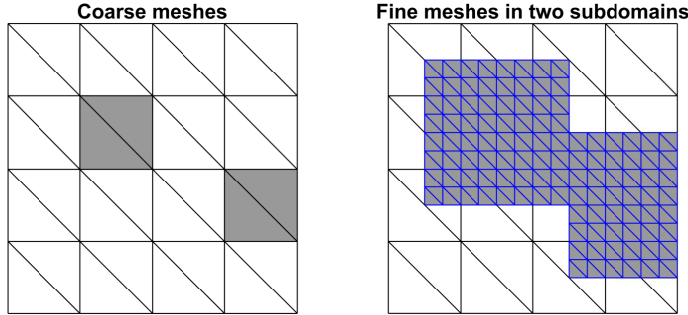


Fig. 2: Construction of an overlapping domain decomposition. Example and figure taken from [20, Example 30].

where λ_H is the smallest eigenvalue of $\mathcal{A}(\cdot, \cdot)$ in V_H , $\|\cdot\|_{\mathcal{A}}$, $\|\cdot\|_{A^{-1}}$, and $\|\cdot\|_{B^{-1}}$ are the norms induced by $\mathcal{A}(\cdot, \cdot)$, A^{-1} , and B^{-1} , respectively, and $c_d > 0$ is a constant independent of the mesh sizes h, H . For any $v \in V_h$ satisfying $\langle u_*, v \rangle_2 = 0$ and $\|v\|_{B^{-1}} = 1$, the Cauchy–Schwarz inequality yields

$$\langle B^{-1}u_*, v \rangle_2 = \langle B^{-1}u_* - \lambda_H^{-1}u_*, v \rangle_2 \leq \|v\|_{A^{-1}} \|B^{-1}u_* - \lambda_H^{-1}u_*\|_{\mathcal{A}} \leq c_d^2 \lambda_1^{-1/2} H.$$

By the variational representation (35) of φ ,

$$\cos \varphi = \sup_{\langle u_*, v \rangle_2 = 0} \frac{\langle B^{-1}u_*, v \rangle_2}{\|v\|_{B^{-1}} \|u_*\|_{B^{-1}}} \leq \frac{c_d^2 \lambda_1^{-1/2} H}{\|u_*\|_{B^{-1}}} \leq c_d^3 H. \quad (39)$$

As c_d is independent of h, H , it follows that $\cos \varphi = \mathcal{O}(H)$ as $H \rightarrow 0$.

5.2 Mixed-precision preconditioners

In this section, we study the condition (35) when using mixed-precision preconditioners as proposed in [11]. For this purpose, we consider two levels of precision: a working precision and a lower precision, for example, IEEE double and single precision. The preconditioner is constructed in lower precision while the rest of the computations are carried out in working precision. For simplicity, the effects of round-off errors in working precision are ignored.

Consider the Cholesky factorization $A = LL^T$, and let \widehat{L} be the Cholesky factor computed in lower precision. We define the preconditioner B as $B^{-1}x := \widehat{L}^{-T}(\widehat{L}^{-1}x)$, which is implemented by solving two triangular linear systems by performing forward and backward substitution in lower precision. By [11, Lemma 3], B^{-1} is a high-quality preconditioner for A , which satisfies

$$\|I - A^{1/2}B^{-1}A^{1/2}\| \leq \frac{\epsilon_l}{1 - \epsilon_l}$$

where we assume $\epsilon_l := 4n(3n+1)(\lambda_n/\lambda_1)\mathbf{u}_l < 1$ and \mathbf{u}_l denotes unit roundoff in lower precision. Note that

$$1 - \|I - A^{1/2}B^{-1}A^{1/2}\| \leq \lambda_{\min}(B^{-1}A) \leq \lambda_{\max}(B^{-1}A) \leq 1 + \|I - A^{1/2}B^{-1}A^{1/2}\|.$$

Using the bound (14) for $\cos \varphi$, it follows that

$$\cos^2 \varphi \leq 1 - \kappa_\nu^{-1} = 1 - \frac{\lambda_{\min}(B^{-1}A)}{\lambda_{\max}(B^{-1}A)} \leq 1 - \frac{1 - \frac{\epsilon_l}{1-\epsilon_l}}{1 + \frac{\epsilon_l}{1-\epsilon_l}} = 2\epsilon_l.$$

Usually $\epsilon_l \ll 1$ and, hence, $\cos \varphi \leq \sqrt{2\epsilon_l}$ is close to zero. This implies that a random starting vector nearly always satisfies the condition (35). In contrast, the condition $\lambda(u_0) < \lambda_2$ required by the classical analysis of PINVIT does not enjoy any benefit from such a high-quality preconditioner.

6 Numerical experiments

In this section, we present some numerical experiments to provide insight into the behavior of φ and a comparison between our initial condition (29) and the classical condition $\lambda(u_0) \in [\lambda_1, \lambda_2)$. All numerical experiments in this section have been implemented in Matlab 2022b and were carried out on an AMD Ryzen 9 6900HX Processor (8 cores, 3.3–4.9 GHz) and 32 GB of RAM.

6.1 Laplace eigenvalue problems

The experiments in this section target the smallest eigenvalue for the Laplacian eigenvalue problem with zero Dirichlet boundary condition on the unit square $\Omega = [0, 1]^2$:

$$\begin{aligned} -\Delta u &= \lambda u & \text{in } \Omega, \\ u &= 0 & \text{on } \partial\Omega, \end{aligned} \tag{40}$$

We will consider two different scenarios:

AGMG Five-points finite difference discretization of (40) on a regular grid of grid size h , together with an AGMG preconditioner,

DDM Piecewise linear finite element discretization of (40) on a regular mesh of mesh width h , as shown in Example 1, together with a DDM preconditioner.

Detailed descriptions of AGMG (aggregation-based algebraic multigrid) preconditioners can be found in [13, 19]; we use the implementation from [18] (release 4.2.2). For DDM, we use the setting described in Example 1; a two-level overlapping domain decomposition preconditioner with an overlapping ratio of 0.5 is applied. Note that in the latter case, we actually solve a generalized eigenvalue problem $A - \lambda M$, see Remark 1, with M representing the mass matrix from the finite element method.

Table 1: Behavior of φ for Laplacian eigenvalue problems with AGMG and DDM preconditioners.

AGMG					
h	2^{-6}	2^{-7}	2^{-8}	2^{-9}	2^{-10}
$\cos^2 \varphi$	0.0331	0.0192	0.0117	0.0064	0.0033
$1 - \kappa_\nu^{-1}$	0.6200	0.6260	0.6352	0.6378	0.6390
χ	0.0534	0.0307	0.0184	0.0101	0.0051
DDM with $H = 2^{-2}$					
h	2^{-4}	2^{-5}	2^{-6}	2^{-7}	2^{-8}
$\cos^2 \varphi$	0.1961	0.1935	0.1915	0.1905	0.1901
$1 - \kappa_\nu^{-1}$	0.8221	0.8201	0.8189	0.8182	0.8178
χ	0.2386	0.2360	0.2339	0.2328	0.2324
DDM with $h = 2^{-8}$					
H	2^{-2}	2^{-3}	2^{-4}	2^{-5}	2^{-6}
$\cos^2 \varphi$	0.1901	0.0720	0.0202	0.0052	0.0013
$1 - \kappa_\nu^{-1}$	0.8178	0.8213	0.8242	0.8278	0.8320
χ	0.2324	0.0877	0.0246	0.0063	0.0016

6.1.1 Behavior of φ

The purpose of the first experiment is to study the angle of distortion φ . A small value of $\cos \varphi$ is favorable for our theory, because this implies that the condition on the initial vector becomes loose. We let $A = -\Delta_h$ denote the discretization of the Laplacian and B denote the preconditioner. For either of the two scenarios described above, the preconditioner is only available implicitly, through matrix-vector products with B^{-1} . The ratio κ_ν can be obtained by computing the smallest and largest eigenvalues of $-B^{-1}\Delta_h$ with the Lanczos method. The definition of the angle φ requires the computation of both Bu_* and $B^{-1}u_*$. While the second computation is straightforward, the first computation is not, because B is not explicitly available. Instead of the matrix-vector multiplication Bu_* , we solve the linear system $B^{-1}z = u_*$ using the preconditioned conjugate gradient method with $-\Delta_h$ as the preconditioner.

Defining

$$\chi := \frac{\cos^2 \varphi}{1 - \kappa_\nu^{-1}},$$

the bound (14) is equivalent to $\chi \leq 1$. From the numerical results in Table 1, one observes that χ is significantly smaller than 1, demonstrating that the bound (14) is not sharp. Table 1 confirms our theoretical result $\cos \varphi = \mathcal{O}(H)$ from (39). For the AGMG preconditioner, it can be observed that $\cos^2 \varphi = \mathcal{O}(h)$, a very favorable behavior.

6.1.2 Empirical probability tests

In most practical situations, PINVIT is used with a random initial vector u_0 . Therefore it is of interest to measure the empirical success probability for our condition $\text{dist}_B(u_0, u_*) < \varphi$ and for the condition $\lambda(u_0) < \lambda_2$ required by [10].

Table 2: Empirical success probabilities for Laplacian eigenvalue problems with AGMG and DDM preconditioners.

AGMG					
h	2^{-6}	2^{-7}	2^{-8}	2^{-9}	2^{-10}
$\lambda(u_0) < \lambda_2$	0%	0%	0%	0%	0%
$\text{dist}_B(u_0, u_*) < \varphi$	44.8%	53.7%	62.1%	67.9%	77.3%
DDM with $H = 2^{-2}$					
h	2^{-4}	2^{-5}	2^{-6}	2^{-7}	2^{-8}
$\lambda(u_0) < \lambda_2$	0.5%	0%	0%	0%	0%
$\text{dist}_B(u_0, u_*) < \varphi$	16.9%	7.2%	4.8%	1.3%	1.2%
DDM with $h = 2^{-8}$					
H	2^{-2}	2^{-3}	2^{-4}	2^{-5}	2^{-6}
$\lambda(u_0) < \lambda_2$	0%	0%	0%	0%	0%
$\text{dist}_B(u_0, u_*) < \varphi$	0.9%	11.1%	41.1%	71.3%	85.8%

It is tempting to choose a Gaussian random vector u_0 , but such a choice is unfortunate—it yields an empirical success probability close to zero for both conditions. A Gaussian random vector tends to be highly oscillatory, whereas the eigenvector u_* is typically very smooth. We address this issue by using a smoother multivariate normal random vector. As the inverse Laplacian effects smoothing, it makes sense to choose $u_0 \sim \mathcal{N}(0, B^{-2})$, which can be computed as $u_0 = B^{-1}\omega$ for a Gaussian random vector ω . Using 1000 independent random trials, we report the empirical success probabilities in Table 2, which impressively show the superiority of our condition on the initial vector.

6.2 Mixed-precision preconditioners for kernel matrices

Following the setting in [11, Section 5.4], we perform experiments with the mixed-precision preconditioner from Section 5.2 for targeting the smallest eigenvalues of a kernel matrix. Choosing independent Gaussian random vectors $x_1, \dots, x_n \in \mathbb{R}^n$, we consider the Laplacian kernel matrix defined by

$$(A)_{ij} = \exp\left(\frac{-\|x_i - x_j\|}{2}\right), \quad i, j = 1, \dots, n.$$

Similarly, choosing another set of independent Gaussian random vectors $y_1, \dots, y_n \in \mathbb{R}^n$ and $K(x, y) = (x^\top y + 1)^3$, we consider the complex kernel matrix defined by

$$(A)_{ij} = K(x_i, x_j) + K(y_i, y_j) + \Im(K(x_i, y_j) - K(y_i, x_j)).$$

In both cases, we choose B be the preconditioner obtained from performing the Cholesky factorization of A in single precision. As in the previous section, we measured the empirical success probability for $\text{dist}_B(u_0, u_*) < \varphi$ and $\lambda(u_0) < \lambda_2$. We choose u_0

Table 3: Empirical success probabilities for dense kernel matrices with mixed-precision preconditioner.

n	Laplacian Kernel				Complex Kernel			
	512	1024	2048	4096	512	1024	2048	4096
$\lambda(u_0) < \lambda_2$	0%	0%	0%	0%	0%	0%	0%	0%
$\text{dist}_B(u_0, u_*) < \varphi$	100%	100%	100%	100%	96.8%	97.9%	100%	100%

to be a Gaussian random vector, set $n \in \{512, 1024, 2048, 4096\}$. For each n , we verify the initial conditions on u_0 by sampling 1000 independent random initial vectors, and collect the results in Table 3. With such effective mixed-precision preconditioners, our condition on the initial vector achieves nearly 100% success probability, whereas the condition $\lambda(u_0) < \lambda_2$ appears to be never satisfied.

7 Conclusions

In this work, we have shown that a variant of PINVIT enjoys a global convergence guarantee (formulated in terms of the angle of distortion) that is observed to be significantly better than the one required by Neymeyr’s classical analysis of PINVIT in case of two classes of preconditioners. The tools developed in this work, especially the connection to Riemannian steepest descent, are potentially useful for developing and analyzing extensions, including accelerated methods in the spirit of [3, 9, 20, 23].

Statements and Declarations

- Funding: FA was supported by the SNSF under research project 192363, BV was supported in part by the SNSF under research project 192129.
- Author contributions: All authors contributed equally to the paper.
- Code availability: Scripts to reproduce numerical results are publicly available at <https://github.com/nShao678/Improved-convergence-of-PINVIT>.
- Conflict of interests: Not applicable.

References

- [1] Absil, P.-A., Mahony, R., Sepulchre, R.: Optimization Algorithms on Matrix Manifolds, p. 224. Princeton University Press, Princeton, NJ (2008). <https://doi.org/10.1515/9781400830244>
- [2] Alimisis, F., Vandereycken, B.: Geodesic Convexity of the Symmetric Eigenvalue Problem and Convergence of Steepest Descent. *J. Optim. Theory Appl.* **203**(1), 920–959 (2024) <https://doi.org/10.1007/s10957-024-02538-8>
- [3] Alimisis, F., Vary, S., Vandereycken, B.: A Nesterov-style accelerated gradient descent algorithm for the symmetric eigenvalue problem. arXiv preprint: 2406.18433 (2024) <https://doi.org/10.48550/arXiv.2406.18433>

- [4] Alimisis, F., Davies, P., Vandereycken, B., Alistarh, D.: Distributed principal component analysis with limited communication. In: Ranzato, M., Beygelzimer, A., Dauphin, Y., Liang, P.S., Vaughan, J.W. (eds.) *Advances in Neural Information Processing Systems*, vol. 34, pp. 2823–2834. Curran Associates, Inc., Red Hook, NY, USA (2021). https://proceedings.neurips.cc/paper_files/paper/2021/file/1680e9fa7b4dd5d62ece800239bb53bd-Paper.pdf
- [5] Boumal, N.: *An Introduction to Optimization on Smooth Manifolds*, p. 338. Cambridge University Press, Cambridge (2023)
- [6] Brenner, S.C., Scott, L.R.: *The Mathematical Theory of Finite Element Methods*, 3rd edn. *Texts in Applied Mathematics*, vol. 15, p. 397. Springer, New York (2008). <https://doi.org/10.1007/978-0-387-75934-0>
- [7] Briggs, W.L., Henson, V.E., McCormick, S.F.: *A Multigrid Tutorial*, 2nd edn., p. 193. Society for Industrial and Applied Mathematics (SIAM), Philadelphia, PA (2000). <https://doi.org/10.1137/1.9780898719505>
- [8] Golub, G.H., Van Loan, C.F.: *Matrix Computations*, 4th edn. *Johns Hopkins Studies in the Mathematical Sciences*, p. 756. Johns Hopkins University Press, Baltimore, MD (2013)
- [9] Knyazev, A.V.: Toward the optimal preconditioned eigensolver: locally optimal block preconditioned conjugate gradient method. vol. 23, pp. 517–541 (2001). <https://doi.org/10.1137/S1064827500366124>
- [10] Knyazev, A.V., Neymeyr, K.: A geometric theory for preconditioned inverse iteration. III. A short and sharp convergence estimate for generalized eigenvalue problems. vol. 358, pp. 95–114 (2003). [https://doi.org/10.1016/S0024-3795\(01\)00461-X](https://doi.org/10.1016/S0024-3795(01)00461-X)
- [11] Kressner, D., Ma, Y., Shao, M.: A mixed precision LOBPCG algorithm. *Numer. Algorithms* **94**(4), 1653–1671 (2023) <https://doi.org/10.1007/s11075-023-01550-9>
- [12] Kyng, R., Sachdeva, S.: Approximate Gaussian elimination for Laplacians—fast, sparse, and simple. In: *57th Annual IEEE Symposium on Foundations of Computer Science—FOCS 2016*, pp. 573–582. IEEE Computer Soc., Los Alamitos, CA (2016)
- [13] Napov, A., Notay, Y.: An algebraic multigrid method with guaranteed convergence rate. *SIAM J. Sci. Comput.* **34**(2), 1079–1109 (2012) <https://doi.org/10.1137/100818509>
- [14] Nesterov, Y.: A method for solving the convex programming problem with convergence rate $O(1/k^2)$. *Dokl. Akad. Nauk SSSR* **269**(3), 543–547 (1983)

- [15] Neymeyr, K.: A geometric theory for preconditioned inverse iteration. I. Extrema of the Rayleigh quotient. *Linear Algebra Appl.* **322**(1-3), 61–85 (2001) [https://doi.org/10.1016/S0024-3795\(00\)00239-1](https://doi.org/10.1016/S0024-3795(00)00239-1)
- [16] Neymeyr, K.: A geometric theory for preconditioned inverse iteration. II. Convergence estimates. *Linear Algebra Appl.* **322**(1-3), 87–104 (2001) [https://doi.org/10.1016/S0024-3795\(00\)00236-6](https://doi.org/10.1016/S0024-3795(00)00236-6)
- [17] Neymeyr, K.: A posteriori error estimation for elliptic eigenproblems. *Numer. Linear Algebra Appl.* **9**(4), 263–279 (2002) <https://doi.org/10.1002/nla.272>
- [18] Notay, Y.: AGMG software and documentation. <http://agmg.eu>
- [19] Notay, Y.: An aggregation-based algebraic multigrid method. *Electron. Trans. Numer. Anal.* **37**, 123–146 (2010)
- [20] Shao, N., Chen, W.: Riemannian acceleration with preconditioning for symmetric eigenvalue problems. arXiv preprint: 2309.05143 (2023) <https://doi.org/10.48550/arXiv.2309.05143>
- [21] Shao, N., Chen, W., Bai, Z.: EPIC: a provable accelerated eigensolver based on preconditioning and implicit convexity. *SIAM J. Matrix Anal. Appl.* (To appear) (2024) <https://doi.org/10.48550/arXiv.2401.11786>
- [22] Smith, S.T.: Optimization techniques on Riemannian manifolds. In: *Hamiltonian and Gradient Flows, Algorithms and Control*. Fields Inst. Commun., vol. 3, pp. 113–136. Amer. Math. Soc., Providence, RI (1994)
- [23] Stathopoulos, A., McCombs, J.R.: PRIMME: preconditioned iterative multi-method eigensolver—methods and software description. *ACM Trans. Math. Software* **37**(2) (2010) <https://doi.org/10.1145/1731022.1731031>
- [24] Toselli, A., Widlund, O.: *Domain Decomposition Methods—algorithms and Theory*. Springer Series in Computational Mathematics, vol. 34, p. 450. Springer, Berlin (2005). <https://doi.org/10.1007/b137868>
- [25] Trefethen, L.N., Bau, D. III: *Numerical Linear Algebra*, p. 361. Society for Industrial and Applied Mathematics (SIAM), Philadelphia, PA (1997). <https://doi.org/10.1137/1.9780898719574>
- [26] Xu, J.: Iterative methods by space decomposition and subspace correction. *SIAM Rev.* **34**(4), 581–613 (1992) <https://doi.org/10.1137/1034116>